Eur. Phys. J. D **24**, 215–218 (2003)
DOI: 10.1140/epjd/e2003-00149-x

THE EUROPEAN PHYSICAL JOURNAL D

Spectroscopic manifestations of phase changes in $CaAr_n$ clusters: finite size effects

F. Calvo[1,a], F. Spiegelman[1], M.A. Gaveau[2], M. Briant[2], P.R. Fournier[2], J.M. Mestdagh[2], and J.P. Visticot[2]

[1] Laboratoire de Physique Quantique[b], IRSAMC, Université Paul Sabatier, 118 route de Narbonne, 31062 Toulouse Cedex, France
[2] Laboratoire Francis Perrin[c], CEA/DRECAM/Service des Photons, Atomes et Molécules, CEN Saclay, 91191 Gif-sur-Yvette Cedex, France

Received 10 September 2002
Published online 3 July 2003 –

Abstract. The finite temperature optical spectroscopy of $CaAr_n$ clusters in the range $6 \leq n \leq 146$ is investigated using a Diatomics-In-Molecule (DIM) Hamiltonian and classical parallel tempering Monte Carlo simulations. The absorption spectrum is calculated in the vertical approximation at various temperatures between 2 K and 50 K. Several typical situations are reported. $CaAr_6$ shows a strong thermal broadening and shift of the spectral lines, possibly associated with isomerization. $CaAr_{13}$ only shows some broadening. $CaAr_{37}$ exhibits features corresponding to coexisting isomers at low temperature. Finally, the abrupt changes in the absorption spectrum in $CaAr_{146}$ at about 20 K are indicative of surface diffusion.

PACS. 36.40.Mr Spectroscopy and geometrical structure of clusters – 36.40.Ei Phase transitions in clusters – 36.40.Vz Optical properties of clusters

1 Introduction

From the experimental point of view, spectroscopy provides a unique tool to investigate the properties of clusters. It has widely been used to provide insight into the structural, electronic and dynamical properties. Recently, spectroscopy techniques have been applied to study the thermodynamical properties of metal clusters and more specifically their phase changes corresponding to the solid-liquid transition [1]. Van der Waals clusters and in particular rare-gas clusters have been widely used as model objects to develop the concepts of phase changes in finite systems [2] and also as benchmarks for simulations. Adding a chromophore impurity to probe the properties of rare-gas clusters is also a common technique. It is the basis of most studies of van der Waals complexes or impurities in helium clusters. Van der Waals complexes are also interesting to favor or mediate chemical reactions such as in Cluster Isolated Chemical Reaction (CICR) experiments [3–5]. In most of these experiments, spectroscopy is a valuable way of characterizing the reactants, the products and even now to follow the processes at the femtosecond scale [6]. In the present paper, we are interested in the possibility of using spectroscopy of a chromophore to characterize the structure and phase changes in argon clusters. This idea is not new, and was the main motivation of early experimental works on benzene [7] and dichloroanthracene [8] in argon clusters. The simplest case consists of an atomic chromophore, for which several theoretical studies have been achieved, especially for alkalis [9–12]. We have recently carried out simulations of the photoabsorption spectrum for large $CaAr_n$ clusters in the range $n = 200-400$ [15]. Here we focus on smaller sizes, looking at the temperature dependence of the spectra in more details. Our aim is to address the possible spectroscopic signatures of isomerization and phase changes in these systems, and to investigate the complex finite-size effects, in a fashion similar to recent other theoretical works [13,14].

After briefly presenting the Hamiltonian and numerical procedure used in this work, we discuss our results in Section 3. We finally summarize and conclude in Section 4.

2 Model and method

The interaction of the calcium atom in its ground state $4s^2$ configuration, with n argon atoms is taken as a sum of pairwise potentials:

$$E_0(\mathbf{R}) = \sum_{i=1}^{n} V_0^{\mathrm{CaAr}}(r_{0i}) + \sum_{1 \leq i < j \leq n} V_0^{\mathrm{ArAr}}(r_{ij}) \quad (1)$$

where $V_0^{\mathrm{CaAr}}(r)$ and $V_0^{\mathrm{ArAr}}(r)$ are the Ca–Ar and Ar–Ar diatomics van der Waals potentials, and where the Ca atom has label 0. The excited states are the eigenvectors

[a] e-mail: florent@irsamc.ups-tlse.fr
[b] UMR 5626, CNRS
[c] CNRS-URA-2453

of a 12×12 Diatomics-In-Molecule (DIM) Hamiltonian expressed in the basis of perturbed atomic configurations $\phi_{\mu\chi\zeta}$ with a hole in one $4s$ orbital of Ca (with spin χ), and an excited electron in one of the $4p$ orbitals labelled by their orientation $\mu = x, y, z$ and spin ζ:

$$\begin{aligned} H_{\mu\zeta\chi,\mu'\zeta\chi} &= e_0\delta_{\mu\mu'} \\ &\quad + \sum_{i=1}^{n}\sum_{\lambda=1}^{3}\rho^i_{\lambda\mu}\rho^i_{\lambda\mu'}\left[V_\lambda^{\mathrm{CaAr}}(r_i) - K_\lambda^{\mathrm{CaAr}}(r_i)\delta_{\zeta\chi}\right] \\ H_{\mu\zeta\chi,\mu'\chi\zeta} &= \sum_{i=1}^{n}\sum_{\lambda=1}^{3}\rho^i_{\lambda\mu}\rho^i_{\lambda\mu'}K_\lambda^{\mathrm{CaAr}}(r_i) \\ &\quad + \sum_{1\le i<j\le n} V_0^{\mathrm{CaAr}}(r_{ij}) \quad \text{if } \chi \neq \zeta. \end{aligned} \tag{2}$$

This model describes both triplet and singlet states correlated with the $4s4p$ configuration, but we will only address here the three higher states of the model, correlated with $4s^1$P (excitation energy 23 652 cm^{-1}). In the above equation, $V_\lambda^{\mathrm{CaAr}}(r)$ and $K_\lambda^{\mathrm{CaAr}}(r)$ are distance-dependent functions representing the mean interaction of an atom in a $4p_\lambda$ orbital ($\lambda = \sigma, \pi$) with a single argon atom, as well as the perturbation of its exchange integral K_{4s4p}. e_0 is the excitation energy of the singlet-triplet average in atomic calcium. $\rho^i_{\mu\nu}$ are unitary matrices, which rotate the $4p$ orbital from the fixed axes to axes aligned with each intracluster Ca–Ar$_i$ direction. Spin-orbit coupling in the $4s4p$ configuration has been included in an atomic-like scheme [15], but its effect is almost non-significant due to its very small value in regard of the singlet-triplet splitting. The omission of the $4s3d$ states, lying in between the triplet and singlet $4s4p$ states in this model, has been discussed in a previous paper [15]. The dipole moments corresponding to absorption between the ground state Φ_0 and the excited states Ψ_m have been determined using an atomic-like approximation

$$D^\nu_{0m} = \langle\Phi_0|\nu|\Psi_m\rangle = d_{sp}(c^m_{\nu\alpha\alpha} + c^m_{\nu\beta\beta}), \tag{3}$$

where $\nu = x$, y, z, and α, β are the eigenstates of the spin projections. d_{sp} is the Ca atom dipole transition integral and $c_{\mu\chi\zeta}$ are the expansion coefficients of the eigenvectors on the basis configurations. More details about the model and the explicit parameterization can be found in [15].

To simulate the absorption spectra, a Monte Carlo random walk was propagated on the ground state potential energy surface (PES) $E_0(\mathbf{R})$ at temperature T, calculating, at each geometry, the transition intensities towards all excited PES's, accumulated in the relevant energy intervals following the vertical transition approximation

$$\mathcal{I}(\varepsilon) = \frac{8\pi^2}{3} \times \frac{\displaystyle\int \sum_m \varepsilon_{0m}(\mathbf{R})|D_{0m}|^2\delta[\varepsilon - \varepsilon_{0m}(\mathbf{R})]\exp[-E_0(\mathbf{R})/k_BT]\mathrm{d}\mathbf{R}}{\displaystyle\int \exp[-E_0(\mathbf{R})/k_BT]\mathrm{d}\mathbf{R}}. \tag{4}$$

$\varepsilon_{0m} = E_m - E_0$ is the transition energy between the ground state and excited state Ψ_m. The clusters were initially set to their lowest energy configuration found by global minimization on the ground state PES using the basin-hopping technique [16].

To reduce the problem of broken ergodicity, we also supplemented the Monte Carlo simulation with the parallel tempering technique [17]. Details on the implementation of this method can be found in [18].

3 Results and discussion

We have selected the CaAr$_n$ clusters with size $n = 6$, 13, 37, and 146, respectively. These sizes span a rather large range and, as will be seen below, can be considered as representative of various situations typical of finite-size effects. Most of the ground state geometries of these clusters are similar to the lowest energy minima of Lennard-Jones clusters [16] with an argon atom substituted by calcium. Due to the larger equilibrium bond length and weaker dissociation energy of Ca–Ar with respect to Ar–Ar [19], the calcium atom is located on surface of the argon cluster, and the structure is locally distorted near the substitution site. The lowest energy structures are represented along the absorption spectra for the four clusters considered here.

The $4s4p$ states yield at most three distinct lines. According to the symmetry (degenerate groups), two of these lines can merge. One state is expected to correspond to a $4p$ orbital pointing toward the cluster. It is significantly perturbed with respect to the atomic line, resulting in a strong shift to the blue, near 24 000 cm^{-1}. The two other orbitals are roughly parallel to the cluster surface, and the spectral lines are less perturbed, possibly shifted to the red [15]. This, along with the possibly questionable AIM assumption, explains the broadness of the band around 24 000 cm^{-1} [15].

CaAr$_6$ is found to have a distorted pentagonal bipyramid geometry with C_{2v} symmetry. At $T = 0$ K, the three non degenerate absorption lines are located at 23 534, 23 771, and 24 093 cm^{-1}. The variations of the absorption spectrum with temperature are shown in Figure 1 in the range 2–50 K with increment $\Delta T = 2$ K. As temperature increases, the three peaks shift and broaden. The splitting between the two lowest energy lines decreases and the two peaks merge around $T \approx 18$ K. At higher temperatures, the spectrum is dominated by this single peak close to the atomic line. However, the occurrence of nearly dissociated Ca–Ar$_n$ configurations at high temperatures $T \geq 35$ K results in a very narrow peak precisely located at the atomic transition energy. The second isomer ($\Delta E = 0.01$ eV higher) is also based on the pentagonal bipyramid with the substituted atom on the C_5 axis. Its vertical spectrum only exhibits two distinct lines at 23 764 and 24 153 cm^{-1}, respectively. This isomer is visited significantly above roughly 20 K, therefore the merging of the peaks may be seen as the signature of isomerization in this cluster.

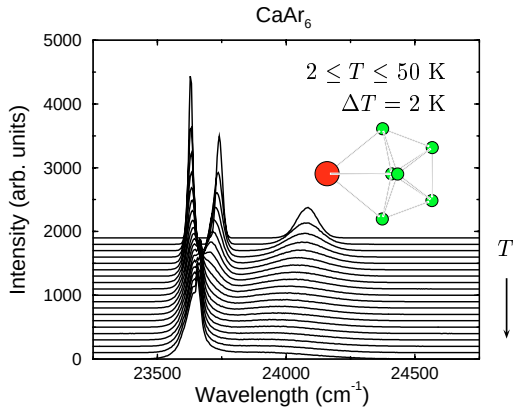

Fig. 1. Temperature evolution of the absorption spectrum for $CaAr_6$.

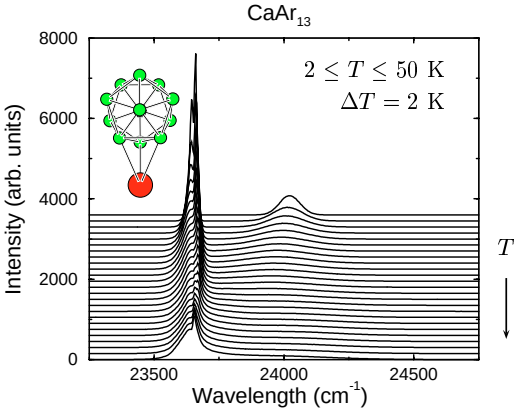

Fig. 2. Same as Figure 1 for $CaAr_{13}$.

$CaAr_{13}$ has the simple structure of a capped Ar_{13} icosahedron with a C_3 symmetry axis. It has two spectral lines at 0 K, located at 23658 (2 degenerate lines) and 24 034 cm^{-1} (1 single line), respectively. This degeneracy is lifted by temperature, and three distinct peaks are observed already at 2 K in Figure 2. As for $CaAr_6$, they merge again into a single broad peak at higher temperatures. The small extra peak at the atomic transition energy is also present. Actual melting in this system involves mostly fluctuations within the argon cluster. However, the insertion of calcium inside this cluster is much less favorable than jumps over the surface, and the absorption spectrum is obviously weakly sensitive to such processes. Thus the monotonic variations (shifts and broadenings) of the spectrum can hardly be used as probes of isomerization in this cluster.

The case of $CaAr_{37}$ is somewhat peculiar, since its global minimum structure is C_{4v} decahedral-based. As in Ar_{38}, geometries based on the icosahedral symmetry are almost as low in energy, and the substitution of argon by calcium even decreases the energy gap: the second minimum is icosahedral and lies about 4×10^{-3} eV above the global minimum. These two isomers are represented in Figure 3 along with the variations of the absorption spectrum with temperature. Their spectral lines show some difference at 0 K. The characteristic peaks of the global

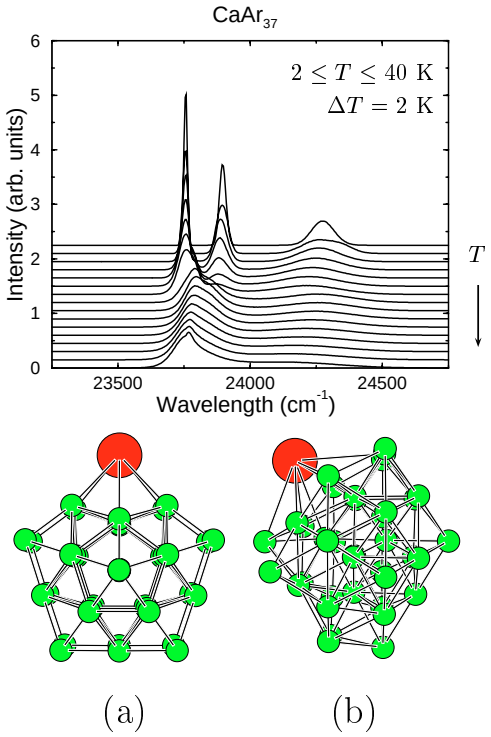

Fig. 3. Upper panel: same as Figure 1 for $CaAr_{37}$. Lower panel: the two lowest energy isomers (a) and (b), $E_b - E_a = +3.96 \times 10^{-3}$ eV.

minimum are located at 23 754, 23 902, and 24 291 cm^{-1}, respectively. The peaks of the icosahedral second minimum are at 23 894, 23 906, and 24 391 cm^{-1}, respectively. While the two formers are close to each other and to the second peak of the global minimum, the latter can be distinctly seen on the spectrum of Figure 3 at $T = 4$ K. Above this temperature, other icosahedral isomers close in energy make this band blur. The two red lines merge and shift to 23 800 cm^{-1} at about $T = 16$ K, where the decahedral minimum gets no longer populated.

$CaAr_{146}$ has a distorted multilayer icosahedral geometry, in which the calcium atom is on a vertex site. Due to the C_5 symmetry, the zero temperature spectrum is made of only two lines, the lowest energy line being twofold degenerate. The finite temperature spectra are shown in Figure 4. The peaks exhibit mainly shifts and broadenings in the range $T \leq 15$ K, but no splitting can be observed on the red component. Above $T = 20$ K, the spectrum undergoes a strong red-shift change resulting into a different two-peak structure. These variations can be interpreted in the light of the known thermodynamic behavior of large icosahedral argon clusters [20]. In these clusters, the solidlike-liquidlike phase change is initiated by surface melting where an increasing number of outer atoms pop out and "float" over the remaining core. Even though this phenomenon does not clearly have a thermodynamical signature on the caloric curves, it starts at temperatures significantly lower than the actual melting point [20,21]. In the present case of $CaAr_{146}$, the smaller bonding of calcium with argon further favors such behavior. Once the

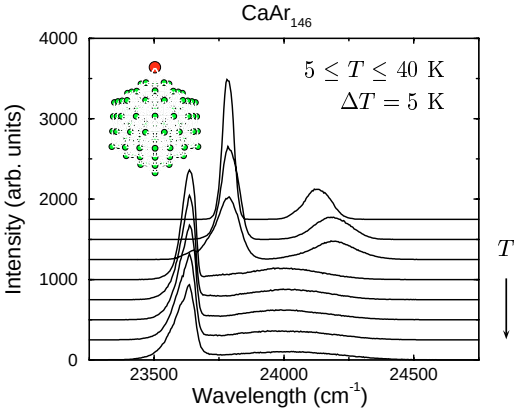

Fig. 4. Same as Figure 1 for $CaAr_{146}$.

calcium atom is able to glide freely over the argon surface, the spectrum remains only weakly sensitive to its precise location. Contrary to $CaAr_{37}$, the coexisting isomers now share essentially the same absorption lines. Therefore, the abrupt change seen in Figure 4 is likely the signature of the first steps of surface melting in this system. However, it should be kept in mind that argon floaters may appear at higher temperatures. As T increases above 20 K, the spectrum becomes essentially singly peaked.

4 Conclusion

In this work, we have investigated the temperature-dependence of the photoabsorption spectrum of $CaAr_n$ clusters with several sizes in the range $6 \leq n \leq 146$. A common feature of all sizes is that the spectra are the same above $T > 30$ K. These spectra show one main peak near 23 600–23 700 cm^{-1}, and also include a spurious thin line associated with evaporation of calcium. At low and intermediate temperatures, changes in the absorption spectra reflect changes in the cluster geometry. The calcium atom is obviously a local probe, and its spectroscopy is mostly sensitive to its immediate neighboring. This is clearly seen in $CaAr_6$, which undergoes isomerization at 20 K, and in $CaAr_{146}$, which undergoes early surface melting also at 20 K. In some cases, the local change of structure results from a more complete cluster rearrangement. This occurs for $CaAr_{37}$, for which the competition between truncated octahedral and icosahedral structures plays an important role below the melting temperature. Such theoretical results could find some experimental proof on ionized, size-selected clusters kept into an electrostatic trap, and would provide an alternative to the structural determination by electron diffraction [22].

A more extensive analysis of these results should include a proper thermodynamical study and its relationship with the various isomers. In addition, some of the features found here at low temperature could be altered with a quantum treatment of the vibrations. These effects are clearly beyond the scope of the present investigation, but could be addressed altogether using an alternative approach such as the superposition approximation [23,24]. Work along these lines is currently in progress.

We thank CALMIP for a generous allocation of computer resources.

References

1. M. Schmidt, R. Kusche, W. Kronmüller, B. von Issendorff, H. Haberland, Phys. Rev. Lett. **79**, 99 (1997)
2. R.S. Berry, in *Large cluster of atoms and molecules*, edited by T.P. Martin, NATO ASI Series E (Kluwer Academic, 1996), Vol. 313, p. 281
3. C. Gée, M.A. Gaveau, J.M. Mestdagh, M.A. Osborne, O. Sublemontier, J.P. Visticot, J. Phys. Chem. **100**, 13421 (1996)
4. J.M. Mestdagh, M.A. Gaveau, C. Gée, O. Sublemontier, J.P. Visticot, Int. Rev. Phys. Chem. **16**, 215 (1997)
5. M.A. Gaveau, C. Gée, J.M. Mestdagh, J.P. Visticot, Comments At. Mol. Phys. **34**, 241 (1999)
6. *Femtosecond real-time spectroscopy of small molecules and clusters*, in Springer Tracts in Modern Physics, edited by E. Schreiber (Springer, Heidelberg, 1998), Vol. 143
7. M.Y. Hahn, R.L. Whetten, Phys. Rev. Lett. **61**, 1190 (1988)
8. U. Even, N. Ben-Horin, J. Jortner, Phys. Rev. Lett. **62**, 140 (1989)
9. C. Tsoo, D.A. Estrin, S.J. Singer, J. Chem. Phys **93**, 7187 (1990); **96**, 7977 (1992)
10. G. Martyna, C. Cheng, M.L. Klein, J. Chem. Phys **95**, 1318 (1991)
11. J.A. Boatz, M.E. Fajardo, J. Chem. Phys. **101**, 3472 (1994)
12. A.V. Nemukhin, B.L. Grigorenko, G.B. Sergeev, Can. J. Phys. **72**, 909 (1994)
13. A.M. Aguado, E. Curotto, Chem. Phys. Lett. **330**, 440 (2000)
14. M. Moseler, H. Häkkinen, U. Landman, Phys. Rev. Lett. **87**, 053401 (2001)
15. M.A. Gaveau, M. Briant, P.R. Fournier, J.-M. Mestdagh, J.-P. Visticot, F. Calvo, S. Baudrand, F. Spiegelman, Eur. Phys. J. D **21**, 153 (2002)
16. D.J. Wales, J.P.K. Doye, J. Phys. Chem. A **101**, 5111 (1997)
17. R.H. Swendsen, J.-S. Wang, Phys. Rev. Lett. **57**, 2607 (1986)
18. J.P. Neirotti, F. Calvo, D.L. Freeman, J.D. Doll, J. Chem. Phys. **112**, 10340 (2000)
19. The parameters of present potential yield D_e = 100.8 cm^{-1}, r_e = 3.7 Å for Ar–Ar, D_e = 70 cm^{-1}, re = 4.95 Å for Ca–Ar
20. H.-P. Cheng, R.S. Berry, Phys. Rev. A **45**, 7969 (1992)
21. J.P.K. Doye, D.J. Wales, J. Chem. Phys. **102**, 9659 (1995)
22. M. Maier-Borst, D.B. Cameron, M. Rokni, J.H. Parks, Phys. Rev. A **59**, R3162 (1999)
23. F.H. Stillinger, T.A. Weber, Phys. Rev. A **25**, 978 (1982)
24. F. Calvo, J.P.K. Doye, D.J. Wales, J. Chem. Phys. **114**, 7312 (2001)